

Combined Active Islanding Detection Method for Grid-connected Photovoltaic System

WEI Quan^{1,2}, WANG Yifei¹, ZHU Jing¹, YIN Xiaogang¹, LIU Zhuang¹

(1. Xi'an High Voltage Apparatus Research Institute Co., Ltd., Xi'an 710077, China;

2. Xi'an Jiaotong University, Xi'an 710049, China)

Abstract: Unintentional islanding phenomenon has been one of the most important problems of grid-connected photovoltaic inverters. To prevent this phenomenon, all kinds of anti-islanding methods have been discussed. This paper presents a combined active islanding detection method, which consists of active frequency drift method and automatic phase-shift method. The traditional active anti-islanding methods of grid-connected PV inverters bear nondetection zone possibilities for certain paralleled RLC loads. The combined method shows islanding detection ability effectively, and it can eliminate nondetection zones even in the worst case conditions. Simulation in different load conditions is performed for verification.

Key words: anti-islanding method; photovoltaic inverter; active frequency drift; automatic phase shift; nondetection zone

CLC number: TM56

Document code: A

Article No.:1001-1609(2014)10-0037-06

0 Introduction

The development of grid-connected photovoltaic (PV) inverters draws attention to islanding phenomenon. The islanding condition refers to that situation in which PV inverters continue supplying a portion of the utility system even though it is isolated from the remainder of the utility system^[1]. Islanding is undesirable because it can cause safety problems to the related equipments or the maintenance staff^[2].

Generally speaking, islanding detection methods (IDM) are classified into passive IDMs and active IDMs^[3-8]. The circuit for assessing IDMs of grid-connected inverters is shown in Fig.1. As a basic passive IDM, under/over voltage protection (UVP/OVP), and under/over frequency protection (UFP/OFP) are commonly equipped into grid-connected inverters. These methods monitor the rms value and frequency of the output voltage, and then activate the voltage and frequency relays when these magnitudes exceed the programmed limits. If there is a power unbalance ($\Delta P = P_{load} - P_{PV} \neq 0$ and/or $\Delta Q = Q_{load} - Q_{PV} \neq 0$) when the utility breaker opens, the voltage magnitude and frequency at the point of common coupling (PCC) will drift to a point

where the active power and reactive power of the local load would match that of the inverter. However, such protections fail if the power of the PV system generation and of the loads demand are matched or even slightly mismatched. Other passive IDMs are also proposed to prevent islanding. But passive methods are not widely used due to the difficulty of selecting the trip limits and their sensitivity to noise sources and mains transients^[9].

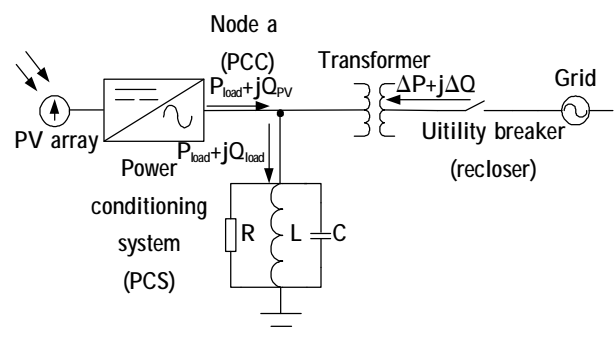


Fig. 1 The circuit of grid-connected photovoltaic inverters

Since passive methods cannot always guarantee detection, active methods are proposed to monitor voltage and frequency of the PCC. Active anti-islanding schemes introduce a disturbance into the PV inverter output current to cause an abnormal condition under islanding conditions. There are three kinds of active islanding detection methods, according to the inverter

output current shown by equation. These are respectively to change magnitude, to change frequency and to change the start phase of the inverter output current^[10]. Much attention has been paid to frequency or phase shift methods.

$$I_{pv} = I_m \sin(2\pi ft + \theta) \quad (1)$$

In this paper, typical active anti-islanding methods: active frequency drift method (AFD)^[11], slip-mode frequency-shift method (SMS)^[12] and automatic phase shift method (APS)^[13], are discussed firstly. All of them bear nondetection zones under certain conditions. Then, a combined active anti-islanding method is introduced to overcome the weaknesses of a single active anti-islanding method. Through analysis and simulation, it is presented that the combined method can eliminate NDZ even in the worse case conditions.

1 Analysis of Active Anti-islanding Methods

1.1 Active frequency drift method

Active frequency drift method (AFD) is shown in Fig.2. AFD method makes the output current of the PV inverter to drift up or down by a parameter chopping fraction (cf) in equation(2).

$$cf = \frac{t_z}{T_u/2} \quad (2)$$

Where T_u is the period of the utility voltage, t_z is the dead time.

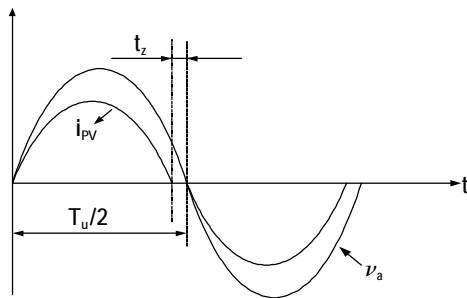


Fig. 2 Inverter output waveform with AFD method (to drift up)

According to phase criterion, if the grid is tripped and the frequency which satisfies equation(3) lies inside the trip limits, the AFD method fails^[14-18].

$$\arg[R^{-1} + (j\omega L)^{-1} + j\omega C]^{-1} = 0.5\omega t_z = 0.5\pi cf \quad (3)$$

If the rated power of the 220 V, 50 Hz inverters is 2 kW. Simulation test was carried out for AFD method. The parameter of the AFD method is $cf=0.05$. Fig.3 and Fig.4 show the responses of magnitude and frequency of the voltage at the PCC. When the grid is tripped,

the magnitude of voltage at the PCC keeps constant, while the frequency is drifted up. According to phase criterion, the stable operating point exits. And simulation result in Fig.4 shows it lies inside the UFP/ OFP trip limits.

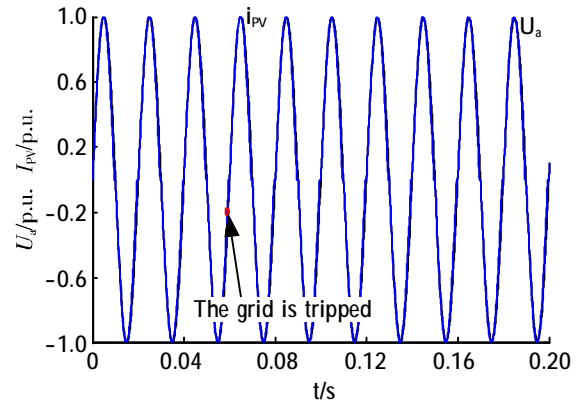


Fig. 3 The responses of the current and the voltage at the PCC of AFD method with $cf=0.05$ ($R=24.2 \Omega$, $L=1.01 \text{ mH}$, and $C=10\ 000 \mu\text{F}$)

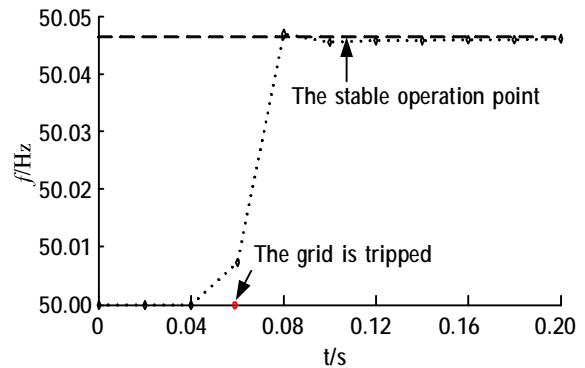


Fig. 4 The response of frequency of AFD method with $cf=0.05$ ($R=24.2 \Omega$, $L=1.01 \text{ mH}$, and $C=10\ 000 \mu\text{F}$)

1.2 Slip-mode frequency-shift method

The SMS method makes the phase angle between the inverter output current and the voltage at the PCC a function of the deviation of the terminal frequency from nominal^[12]. The phase angle of the inverter output current is controlled by the following equation:

$$\theta_{SMS} = \theta_m \sin\left[\frac{\pi}{2} \frac{f(k-1) - 50 \text{ Hz}}{f_m - 50 \text{ Hz}}\right] \quad (4)$$

Where f_m is the frequency at which the maximum phase shift θ_m occurs, $f(k-1)$ is the measured frequency of the previous voltage cycle.

The SMS method don't continuously disturb the inverter output variables, but only start disturbing these variables when they notice that the variable have changed^[19]. The phase angle φ_{load} of the impedance of a parallel RLC load depends on the operating frequency f .

$$\varphi_{load} = \arctan\left[R\left(\frac{1}{2\pi fL} - 2\pi fC\right)\right] \quad (5)$$

The slope of θ_{SMS} line shown in Fig.5 is greater than that of the phase of the load in the region near the grid line frequency^[20]. When the grid is connected, the measured previous cycle frequency is the same with the grid voltage frequency. When the utility breaker is open, even a small disturbance will drive the operating frequency up or down until it satisfies equation(6).

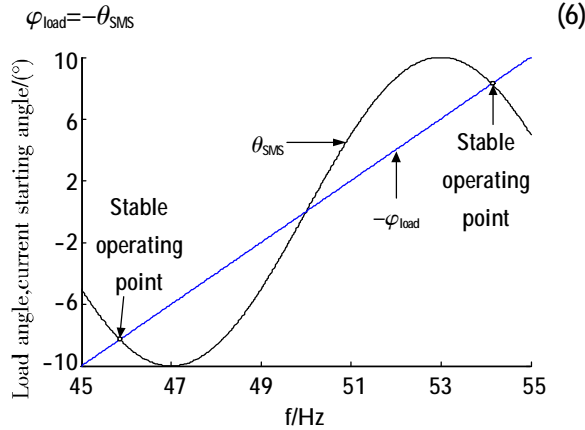


Fig. 5 The phase response of inverter output current and local load

However, if the frequency at which the phase criterion is satisfied lies inside the trip limits, the SMS method fails and that is the reason why nondetection zone exits. So this method can not be always effective under the conditions that the characteristics of the load supplied by the inverter interact with the method and the frequency stabilizes within the UFP/OFP trip limits. As a consequence, this method is not widely used to detect islanding in photovoltaic inverters.

Simulation test was also carried out for SMS method. The parameters of the SMS method are $\theta_m = 10^\circ$ and $f_m = 53$ Hz, and the rated power of the 220 V, 50 Hz inverters is 10 kW. Fig.6 shows the response of frequency of SMS method. When the utility breaker is open, SMS method makes the frequency of the voltage at the PCC drift up. From Fig.6, it shows that the frequency still lies inside the UFP/OFP trip limits at the stable operation point.

1.3 Automatic phase shift method

The APS method is presented to break possible stable operating points of SMS within the UFP-OFP window^[13]. The control function for APS is

$$\theta_{APS}(k) = \frac{1}{\alpha} \cdot \frac{f(k-1) - 50 \text{ Hz}}{50 \text{ Hz}} \cdot 360^\circ + \theta_0(k) \quad (7)$$

Where, α is feedback coefficient; $f(k-1)$ is the measured frequency of the previous voltage cycle.

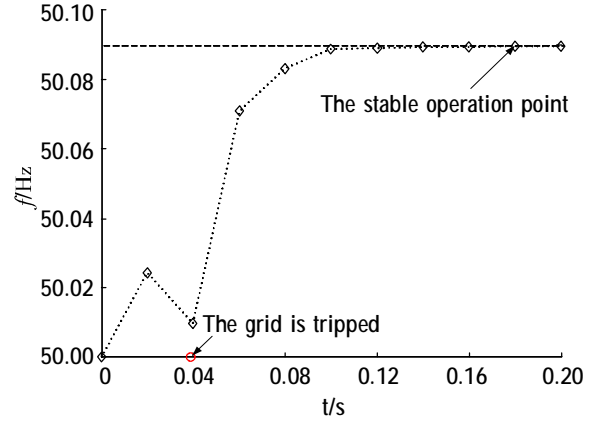


Fig. 6 The response of frequency of SMS method ($R=4.84 \Omega$, $L=1.01$ mH, and $C=10\ 000 \mu\text{F}$)

If the steady state frequency of the voltage at the PCC reaches while the frequency is still inside the trip limits window, the additional phase shift θ_0 will be changed as equation(8).

$$\theta_0(k) = \theta_0(k-1) + \Delta\theta \times \text{sgn}(\Delta f_{ss}) \quad (8)$$

Where, $\Delta\theta$ is the constant; Δf_{ss} is the change of steady-state frequency; $\theta_0(k) = 0$; $\forall k \leq 0$.

$$\text{sgn}(\Delta f_{ss}) = \begin{cases} 1, & \Delta f_{ss} > 0 \\ 0, & \Delta f_{ss} = 0 \\ -1, & \Delta f_{ss} < 0 \end{cases}$$

The APS method can break stable operating points due to positive feedback θ_0 , while the SMS method must operate in an unstable mode. However, the APS method also has a distinct drawback. That is, when the utility trips at the grid line frequency while the resonance frequency of the local load is also the grid line frequency, APS can't break the worst stable operating point for the additional phase shift is equal to zero. Although it is a very special situation, it very likely happens because the inverters are always required to work at the unit power factor. Also, the load resonance frequency is designed to grid line frequency to improve the power quality.

2 The Combined Anti-islanding Method

To overcome the weaknesses of a single anti-islanding method, this paper presents a novel combined active islanding detection method, which consists of active frequency drift method and automatic phase shift method.

The flow diagram of the combined anti-islanding algorithm is shown in Fig.7. The combined method can eliminate the worst case condition. When the grid is

tripped at the worst case condition, the Δf_{ss} is equal to zero, and the resonance frequency of the local load f_0 is equal to the grid line frequency f_g . The combined anti-islanding method can break the stable operation point at the worst case condition by introducing AFD method.

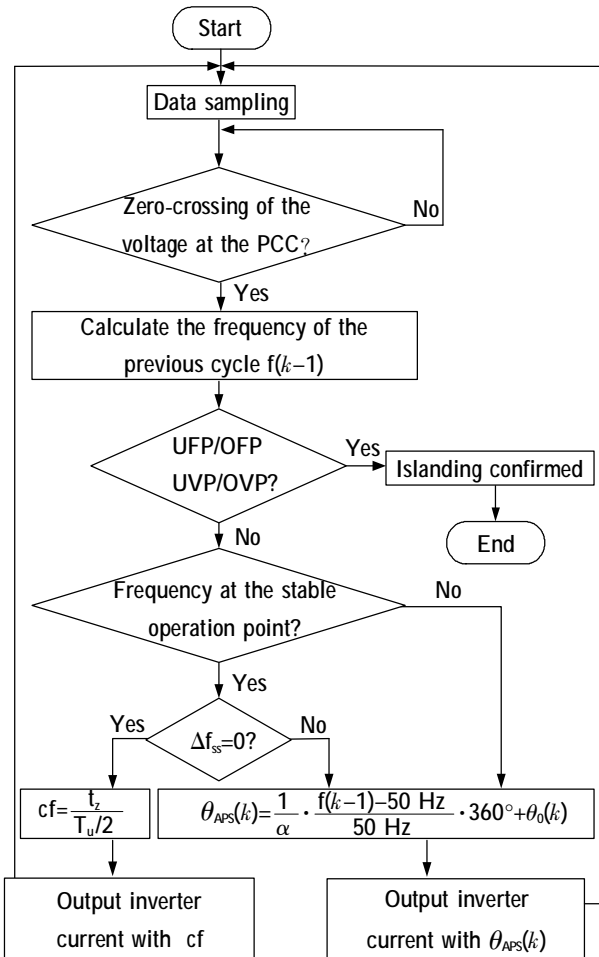


Fig. 7 The program flow of the combined anti-islanding method

3 Simulation Results

When the utility breaker opens, the grid-connected PV inverter operates in islanding mode, and the combined anti-islanding method make the frequency of the output current drift up or down.

The grid-connected PV inverter system shown in Fig.1 was simulated with the combined anti-islanding method in the previous section. The parameters of the combined anti-islanding method are $\alpha=2$, $\Delta\theta=3.6^\circ$, and $cf=0.02$. And the rated power of the 220 V, 50 Hz inverters is 2 kW.

Fig.8-13 show the responses of magnitude and frequency of the voltage at the PCC with different values

of local loads.

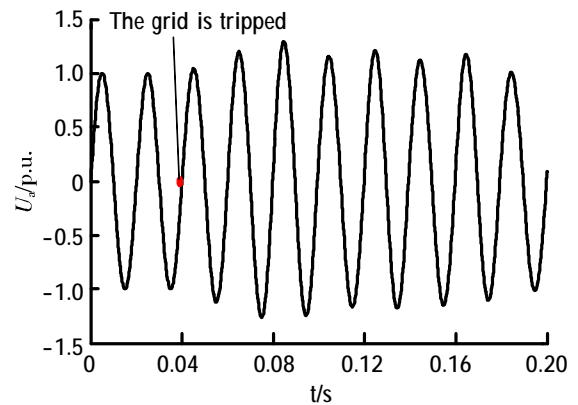


Fig. 8 The responses of the voltage at the PCC of the combined anti-islanding method (R=24.2 Ω, L=1.01 mH, and C=10 000 μF)

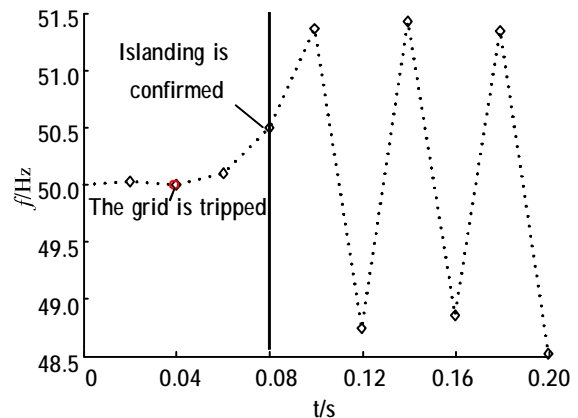


Fig. 9 The response of frequency of the combined anti-islanding method (R=24.2 Ω, L=1.01 mH, and C=10 000 μF)

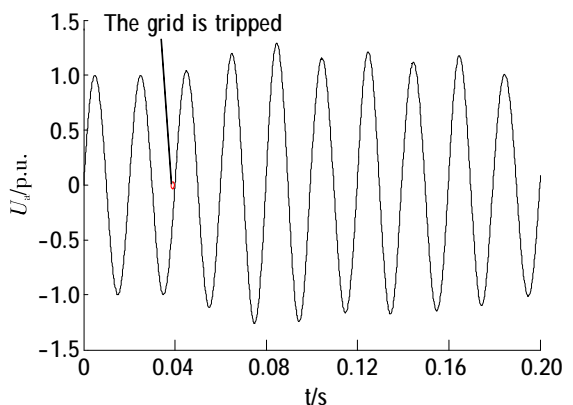


Fig. 10 The responses of the voltage at the PCC of the combined anti-islanding method (R=24.2 Ω, L=1.01 mH, and C=6 800 μF)

If the resonant frequency of the paralleled RLC loads is equal to the grid line frequency, the load is resistive at the grid line frequency. When the grid is tripped at the grid line frequency, the APS method will fail to detect islanding. While the combined anti-islanding method can break the stable operation point

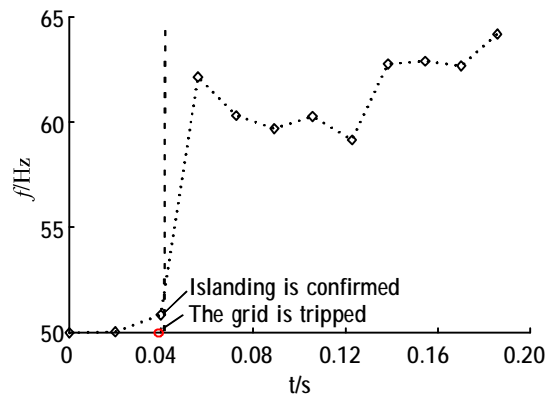


Fig. 11 The response of frequency of the combined anti-islanding method (R=24.2 Ω, L=1.01 mH, and C=6 800 μF)

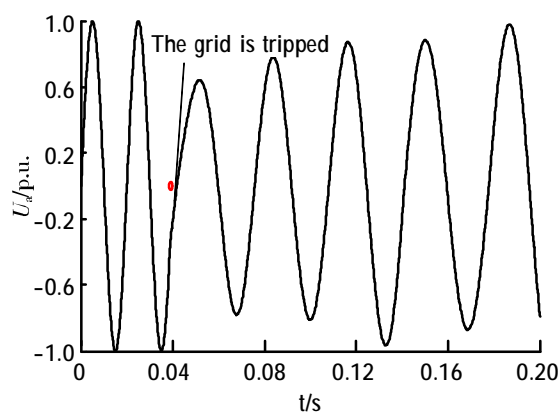


Fig. 12 The responses of the voltage at the PCC of the combined anti-islanding method (R=24.2 Ω, L=3 mH, and C=10 000 μF)

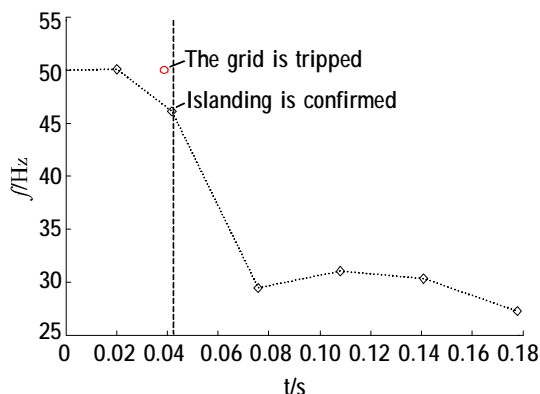


Fig. 13 The response of frequency of the combined anti-islanding method (R=24.2 Ω, L=1.01 mH, and C=6 800 μF)

by introducing AFD method. Simulation result shown in Fig.9 indicates that the combined method can detect islanding in the worst condition.

If the resonant frequency of the paralleled RLC load is larger than the grid line frequency, the load is inductive at the grid line frequency. When the utility breaker opens, the combined anti-islanding method makes the frequency of the output current drift up.

Simulation result shown in Fig.11 indicates the frequency of the voltage at the PCC drifts up when the grid is tripped.

If the resonant frequency of the paralleled RLC load is smaller than the grid line frequency, the load is capacitive at the grid line frequency. When the utility breaker opens, the combined anti-islanding method makes the frequency of the output current drift down. Simulation result shown in Fig.13 indicates the frequency of the voltage at the PCC drifts down when the grid is tripped.

Simulation results show that the combined anti-islanding method can detect islanding within 2 seconds after the grid is tripped in different load conditions. And it also indicates the combined method can eliminate nondetection zones even in the worst case conditions.

4 Conclusions

This paper presents a combined active islanding detection method, which consists of active frequency drift method and automatic phase-shift method. Traditional phase shift methods: AFD, SMS and APS are discussed first. AFD and SMS may fail under certain loads condition according to phase criterion. The APS method is presented to break possible stable operating points of SMS within the UFP-OFP window, but APS can not detect island under the worst condition. The combined anti-islanding method can overcome the weaknesses of a single active anti-islanding method. Simulation results in different load conditions show that the combined anti-islanding method can detect effectively, and it can eliminate nondetection zones even in the worst case condition.

References:

- [1] IEEE Std 929—2000 IEEE recommended practice for utility interface of photovoltaic (PV) systems[S].2000.
- [2] ROPP M E, BEGOVIC M, ROHATGI A. Prevention of islanding in grid-connected photovoltaic systems[J]. Progress in Photovoltaics Research and Applications,1999(7): 39-59.
- [3] YIN Jun, CHANG Liuchen, DIDUCH C.Recent developments in islanding detection for distributed power generation[C]//2004 Large Engineering Systems Conference of Power Engineering.[S.I.]:IEEE, 2004:124-128.

- [4] JEONG J B, KIM H J. Active anti-islanding method for PV system using reactive power control[J]. *Electronics Letters*, 2006, 42(17):1004-1005.
- [5] LIU F, KANG Y, ZHANG Y, et al. Improved SMS islanding detection method for grid-connected converters[J]. *IET Renewable Power Generation*, 2010, 4(1):36-42.
- [6] ZEINELDIN H H, ELSAADANY E F, SALAMA M M A. Islanding detection of inverter-based distributed generation[J]. *IEE Proceedings of Generation, Transmission and Distribution*, 2006, 153(6):644-652.
- [7] MANGO F, LISERRE M, AQUILA D A, et al. Overview of anti-islanding algorithms for PV systems. Part I: Passive methods[C]//*Power Electronics and Motion Control Conference*. [S.l.]: IEEE, 2006:1878-1883.
- [8] MANGO F, LISERRE M, AQUILA D A, et al. Overview of anti-islanding algorithms for PV systems. Part II: Active methods[C]//*Power Electronics and Motion Control Conference*. [S.l.]: IEEE, 2006:1884-1889.
- [9] SANCHIS P, MARROYO L, COLOMA J. Design methodology for the frequency shift method of islanding prevention and analysis of its detection capability[J]. *Prog. Photovolt: Res. Appl.*, 2005(13):409-428.
- [10] YU B, MATSUI M, JUNG Y, et al. A combined active anti-islanding method for photovoltaic systems[J]. *Renewable Energy*, 2008(33):979-985.
- [11] ROPP M E, BEGOVIC M, ROHATGI A. Analysis and performance assessment of the active frequency drift method of islanding prevention[J]. *IEEE Trans. on Energy Conversion*, 1999(14):810-816.
- [12] SMITH G A, ONIONS P A, INFIELD D G. Predicting islanding operation of grid connected PV inverters[J]. *IEE Proceedings of Electric Power Application*, 2000, 147(1):1-6.
- [13] HUNG G K, CHANG C C, CHEN C L. Automatic phase-shift method for islanding detection of grid-connected photovoltaic inverters[J]. *IEEE Trans. on Energy Conversion*, 2003, 18(1):169-173.
- [14] VIEIRA J C M, FREITAS W, XU W, et al. An investigation on the nondetection zones of synchronous distributed generation anti-islanding protection[J]. *IEEE Transactions on Power Delivery*, 2008, 23(2): 593-600.
- [15] ROPP M E, BEGOVIC M, ROHATGI A. Analysis and performance assessment of the active frequency drift method of islanding prevention[J]. *IEEE Transactions on Energy Conversion*, 1999, 14(3):810-816.
- [16] YE Zhihong, KOLWALKAR A, ZHANG Yu, et al. Evaluation of anti-islanding schemes based on nondetection zone concept[J]. *IEEE Transactions on Power Electronics*, 2004, 19(5):1171-1176.
- [17] ZEINELDIN H H, SAADANY E F, SALAMA M M A. Impact of DG interface control on islanding detection and nondetection zones[J]. *IEEE Transactions on Power Delivery*, 2006, 21(3):1515-1523.
- [18] ROPP M E, BEGOVIC M, ROHATGI A, et al. Determining the relative effectiveness of islanding detection methods using phase criteria and nondetection zones [J]. *IEEE Transactions on Energy Conversion*, 2000, 15(3):290-296.
- [19] YU B, MATSUI M, JUNG Y, et al. Modeling and design of phase shift anti-islanding method using nondetection zone[J]. *Solar Energy*, 2007(81):1333-1339.
- [20] LOPES L A C, SUN H. Performance assessment of active frequency drift islanding detection methods [J]. *IEEE Transactions on Energy Conversion*, 2006, 21(1):171-180.

WEI Quan (1979—), male, bachelor, engineer, mainly engaged in RAD of the switchgear and power electronics devices.